20th Australasian Fluid Mechanics Conference
Perth, Australia
5-8 December 2016

Numerical Study of Liquid Transport in Realistic Filter Media

V. Golkarfard[1, 2], B.J. Mullins[2, 3], A.J.C. King[1, 2], S. Abishek[2, 3]

[1]Department of Mechanical Engineering
Curtin University, Western Australia 6102, Australia

[2]Fluid Dynamics Research Group, Curtin Institute of Computing
Curtin University, Western Australia 6102, Australia

[3]Occupation and Environment, School of Public Health
Curtin University, Western Australia 6102, Australia

Abstract

Aerosol filtration is critical to a wide range of industrial process technologies. Although there are many studies which have focused on dust filtration mechanisms, little is known about the behaviour of saturated mist filter systems and associated transport mechanisms within filters. Experimental investigation into internal filter transport of coalesced aerosol is both difficult and time consuming. Therefore, Computational Fluid Dynamics (CFD) methods have the potential to reduce the costs and time required for filter development. Thus, the main objective of this research is to develop numerical models to simulate the liquid transport in representative filter geometries. In this study, three different filter media, fibrous filters, knitted filters, and open-cell foams, will be surveyed. The present study is carried out under two different levels of initial fluid saturation of 20% and 30% in the filter medium. The entrance air flow velocity varies from 0.5 m/s to 5 m/s. OpenFOAM software is used for the numerical calculations. Moreover, a second goal of the research is to understand in detail and at small scales, the various filtration mechanisms. Subsequently the research will investigate velocity and saturation variation, and fluid behaviour after saturation in different filter media types.

Introduction

Filtration processes are needed in a wide range of process industries. In the case of liquid aerosols, such as oil-mists which are typically formed due to various industrial processes, their filtration dynamics differs from solid particle filtration [1]. One of the most commonly used method for treating or removing liquids from gas is filters especially fibrous media [1]. Apart from the structure of filters which categorises them into fibrous, knitted, open-cell foam, filters divide into woven and non-woven media. Furthermore, their wettability characteristics play a key role in evaluation of filters' efficiency and performance and according to these filters are divided into two main category which named oleophilic and oleophobic. In oleophilic media, droplets collect and spread out over the fibre surface and a thin film will be formed. This film will be immediately broken up into an array of droplets due to Plateau-Rayleigh instability. Most of the industrial filters are oleophilic which are relatively well described [2]. On the other hand, in the oleophobic case, captured liquid aerosol do not coat the fibre, and it remains as discrete droplet, unless it moves and contact other droplets which consequently resulted in coalescence or carried through filter by airflow forces. There have been relatively few works that have studied oleophobic filters and the majority of works have only considered droplets on single fibres.
Like most of the engineering research, this filed can be separated into both experimental and numerical studies. Since the main focus of this research is to understanding fluid transport through various filter media, numerical researches are reviewed briefly. In regard to numerical studies, simulations have been developed for single fibre systems, as well as more complicated multi-fibre systems, the most advanced of which approach whole filter simulation. In the case of filter modelling, virtual filter structure has been designed and developed by many researchers which represents non-woven fibre media [3], on the other hand some scientists have tried to simulate realistic filter media by means of imaging filter media [4]. It should be mentioned this method is time consuming, involve many steps, and there is a possibility of altering the media during imaging process. Since transport of liquid within a filter is difficult to observe, many researchers are inclined toward using numerical methods. The predominant method for filtration simulation is applying Finite Volume Method (FVM) of Computational Fluid Dynamics (CFD). These simulations include investigating the effect of fibre diameter on filter permeability [4], fibre orientation on filter performance [5]. Spielman and Goren [6] solved the flow through 3-D arrays of cylinders randomly oriented in all three directions by analytical techniques. Many researchers have studied air flow through filters as well as particle deposition. In 2013, Mead-Hunter et al. [7] have considered the capture and coalescence of liquid droplets in a filter. They used a combination of Lagrangian particle tracking and volume of fluid (VOF) method to simulate the filtering behaviour.

In this work, the behaviour of different initially saturated (20 % and 30%) oil-mist in three different oleophobic filter geometries which are created programmatically (fibrous, knitted, and open-cell foam) is investigated. Different air flow velocities are investigated numerically. The oleophobic filter type is chosen since many oil mist filters are Oleophobic, and these filters have lower saturation and also lower pressure drop throughout the filter – though possibly higher re-entrainment. The main goal of the research is to understand in detail the difference between these realistic filter media from filtration perspective. Subsequently the research will investigate specific effects of variation in saturation and inlet velocity after pre saturation in different filter media types.

Cases Studied

The main purpose of this research is to compare the behaviour of pre saturated oil-mist filters in different geometric configuration, different air flow conditions, and different initial saturation. All the cases are pre-saturated since the simulations are time-consuming, and it would be too computationally expensive to run all simulations from the start (unloaded filter). Figure 1 represents the representative filter geometries.

In this study, all the produced filter geometries have a packing density (solidity) of 2 % with fibre/element diameter of 9 μm and overall dimensions of: 2mm (z), 0.5 mm (x), and 0.5 mm (y). The computational surrounding box domain is 4 mm in the z direction (the length of the filters is 2 mm in z direction) and 0.5 mm in both the x and y directions. The initial pressure drop through the filters

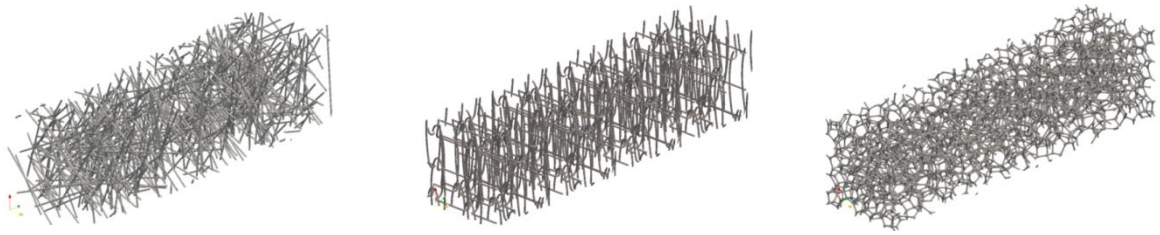

(a) (b) (c)

Figure 1. Filter geometries: (a) Fibrous, (b) Knitted, (c) Open-cell Foam

(with 2 m/s velocity) are 106.2, 76.8, and 94.8 pa for fibrous, knitted, and foam, respectively which provide a basis to compare the performance of the three types of media.

The saturation of the filters is initialised 20% and 30 % of the simulated filter volume with Di-Ethyl-Hexyl-Sebacate (DEHS). It is a monocomponent, non-soluble, colourless and odourless liquid which is suitable for producing stable oil aerosol. It is common lab oil, and also has low vapour pressure, so evaporation can be ignored. In regard to compare these three filter media, the initial distribution of DEHS droplets are similar in all study cases. Figure 2 shows the initial position of droplets for fibrous case with 20% saturation in computational domain as a representative.

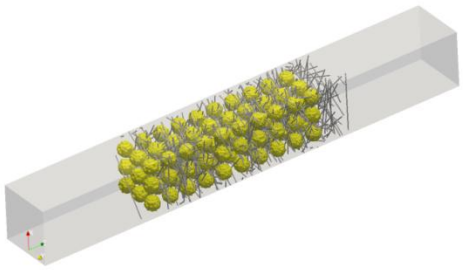

Figure 2. Initial position of distributed droplets

For studying liquid transport, five different face velocities of 0.5, 1, 2, 3, and 5 m/s are prescribed at inlet boundary.

Methodology

In order to capture the gas-liquid interface, the Volume of Fluid (VOF) method is applied [8]. The VOF method is based on the definition of an indicator function which indicates whether the cell is occupied by one fluid or another. In the conventional volume of fluid (VOF) method, the transport equation for an indicator function, representing the volume fraction of one phase (the oil in the case of coalescing filters), is solved simultaneously with the continuity and momentum equations. The governing equations are fully detailed in [8].

To perform the simulations, the open source computational fluid dynamics (CFD) toolbox, OpenFOAM [9], is applied. This software is based on the finite volume method. The solver used was a three-dimensional unsteady solver which utilised the Multidimensional Universal Limiter with Explicit Solutions (MULES) algorithm to handle the transport equation and the Pressure. This solver Split the Operators (PISO) algorithm for the coupled pressure-velocity fields [10].

In order to discretise the computational domain, snappyHexMesh utility is used. The mesh was refined that means the grid spacing is progressively reduced until further decreases made no significant change in the predicted pressure drop for simulations.

In VOF-based methods, since the convergence and stability are strictly dependent on the equation for volume fraction, both time step control and bounded discretisation schemes for divergence terms are employed to overcome these difficulties. Laminar incompressible flow is assumed to prevail inside the solution domain for the face velocities considered in this study (Re_f<15). where Re_f is fibre Reynolds number and defined as:

$$Re_f = \frac{\rho U d_f}{\mu} \quad (1)$$

In this equation, μ ($kg.m^{-1}s^{-1}$) is gas dynamic viscosity, U is face velocity ($m.s^{-1}$), ρ (kg.m^{-3}) is gas density, and d_f (m) is fibre diameter.

In the case of boundary conditions, which play an important role in CFD calculations, it should be stated that the boundary conditions that are required to be exerted on the filter surfaces are velocity and contact angle conditions. The no-slip condition is considered for the surface of the filters since this fibre diameter (9 μm) and face velocities lead to $0.01< Kn_f < 0.05$, and are outside the slip flow regime [11]. Kn_f is fibre's Knudsen number and defined as:

$$Kn = \frac{2\lambda}{d_f} \quad (2)$$

In equation (2), λ is the molecular mean free path in air, and d_f is fibre diameter. Furthermore, effect of contact line velocity on the contact-angle that is not taken into account, and the contact angle which is prescribed at the filter surface was considered as a static one without any changes equal to 120 degrees. The inlet and outlet boundary conditions are placed far from any strong gradients as uniform boundary conditions are applied. For the sides of the computational box, symmetry boundary condition is considered.

We have used symmetry boundary condition for the surrounding sides of the computational box, even though there is no plane of symmetry in a disordered fibrous structure. This boundary condition is considered for the simulations because the overall effects are so, and use of cyclic boundary condition will introduce artificial wall faces on the boundaries.

Validation

To verify the accuracy of computations, the calculation of clean pressure drop is compared against well-established pressure correlation by Spielman and Goren [6]. Since in their work, they just studied fibrous media with various fibre orientation, the clean pressure drop of all simulated filter media with different face velocities is calculated and compared against [6], and is presented by figure 3. This figure, shows the dimensionless pressure drop, or Euler number,Eu $= \frac{\Delta P}{\rho_f U^2}$, as a function of fibre Reynolds number (Re_f).

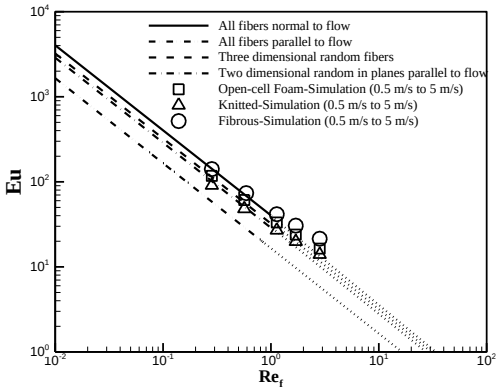

Figure 3. Comparison of predicted clean pressure drop with [6]

It is apparent from the graph that the fibrous filter simulation results adhere to the case which all fibres orientation are normal to flow, while open-cell foam result is similar to three dimensional random fibers. In the case of knitted media, due to its special fibre orientation, it behaves like two dimensional random fibre filter. As can be seen from figure 3, a good agreement exists between the simulations with low face velocities (0.5, 1, and 2 m/s) and [6], while a deviation is clear for cases with 3 and 5 m/s velocities in all simulations. To investigate the underlying reason for this occurrence one should consider the governing laws in fluid pressure drop through porous media. In 1856, Darcy [13] presented a fundamental law which links velocity and pressure drop of a fluid through porous media. Darcy's law can be written as [6] :

$$\Delta P = -\frac{1}{K}\mu U \Delta L \quad (3)$$

Where ΔP (pa) is pressure drop, K (m^{-2}) is permeability, μ ($kg.m^{-1}s^{-1}$) is gas dynamic viscosity, U is interfacial velocity (face velocity) ($m.s^{-1}$), and ΔL (m) is the length of the media. It is widely accepted that Darcy's law is capable to correctly describe the pressure drop of a flow with low velocity in porous media [6], however, by increase in flow velocity, a discrepancy between experimental results and Darcy's law prediction occurs. Forchheimer (1901) related this occurrence to inertial effects and suggested a modified version of Darcy's law with additional term which represents kinetic energy [14] :

$$\Delta P = -\frac{1}{K}\mu U \Delta L + \beta \times (\rho \times U^2) \quad (4)$$

Where β (m^{-1}) is non-Darcy coefficient and ρ ($kg.m^{-3}$) is fluid density. It is worth mentioning that this non-linearity occurs still within the laminar flow regime and is not necessarily related to turbulence [15-17]. Most of the researchers assume that the 1<Re_f <10 is the upper limit for Darcy's law [18].

As can be seen from the figure 3, our numerical results of different media pressure drop adhere to the proposed equation by Darcy (which is the basis of the model presented by [6]) perfectly for low velocity cases (where Reynolds number is less than 1), while the deviation is occurred for higher velocities due to non-linearity of non-Darcy regime.

Results and discussion

In this section, the numerical results for the transport of DEHS droplets through different filter media are presented. Simulations were conducted on nonwoven fibrous, knitted, and open-cell foam media at different initial saturation (20 and 30 %) and inlet velocities: 0.5, 1, 2, 3, and 5 m/s. The physical properties used for fluids are given in Table 1.

Fluid	Density, ρ ($^{kg}/_{m^3}$)	Dynamic viscosity, μ (Pa s)	Surface tension, σ ($^{N}/_{m}$)
DEHS	914	0.025	0.0324
Air	1.1845	1.557×10-5	-

Note: σ represents the surface tension of the liquid–air interface.

Table 1. Physical properties of fluids.

Figure 4 shows simulated values for normalized saturation ($S_{norm.}$) in the filter domain versus inlet velocity. It should be stated that in this figure all the filters have similar diameter of 9 μm with the same solidity of 2 %. In this figure, the calculated numerical data are demonstrated by symbols while the lines show spline fits to these data to aid interpretation. The volume fraction is calculated by:

$$S = \frac{V_l}{V_{void}} \quad (4)$$

Where V_l , is the volume of liquid phase (DEHS) in the filter domain and V_{void} is the summation of the liquid phase volume and gas volume (volume inside the filter not occupied by fibres) and $S_{norm.}$:

$$S_{norm.} = \frac{S}{S_{initial}} \quad (5)$$

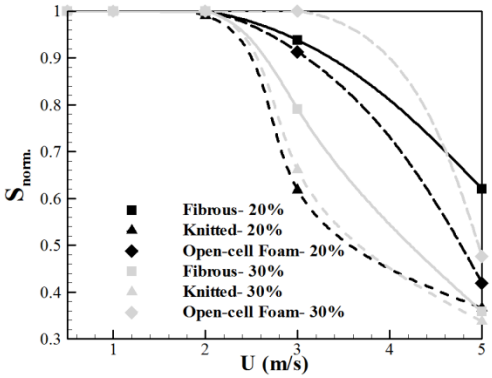

Figure 4. Change in saturation versus velocity

The first point which can be gained from figure 4 is that by increasing inlet velocity, saturation reduces in all different filter media. Furthermore, it is seen that the onset of normalized saturation reduction can be anticipated at velocity around 2.1 m/s for all the filter media except open-cell foam with 30% saturation in which saturation decrease occurs at approximate 3 m/s. The main reason could be that these lower velocities do not provide sufficient force to carry droplets out of filters.

From initial saturation comparison perspective, it is observed that foam and knitted media reach similar level of saturation at steady state by increase in velocity (at 5 m/s velocity), while fibrous filter shows 43.5 % reduction in normalized saturation. It can be reasoned by the fact that increase in initial saturation would increase the possibility of larger droplets formation in filter media which require lower force for moving droplets.

Another interesting result which can be gained from figure 4 is that in all study cases knitted media has the lowest amount of saturation. For better examination of this phenomenon, figure 5 indicates comparative velocity contour and droplet snapshots at 50 unit of dimensionless time ($t^* = \frac{t \times v}{z}$ where t^* is dimensionless time, t is actual time, v is face velocity, and z is filter thickness in z direction) with 1 m/s inlet velocity for all three filter media.

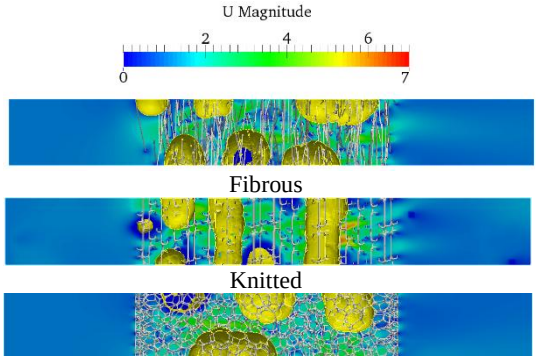

Figure 5. Velocity contour and droplet snapshot for all cases

We can see from figure 5 that knitted media not only provides larger droplets in compare to other filter media, it also produces higher velocity. The main reason for this may likely be due to the filter structural difference in these three filters which results in displacement of centre of mass of retained liquid away from centre of fibre. This increased parameter would decrease the force required to move a droplet [19].

Conclusion

This work has examined the movement of droplets in fibrous, knitted, and open-cell foam media with a range of different face velocities and initial saturation. It was found that by increasing in velocity, liquid volume fraction in the filters reduced though detachment occurs around 2 m/s in all cases except open-cell foam with 30% initial saturation which experiences liquid volume fraction reduction at 3 m/s. Furthermore, it has been shown that foam and knitted media reached approximately similar volume fraction by increasing in initial saturation; however, fibrous media indicated 43.5% decrease by increase in initial saturation. It is worth mentioning that other factors such as initial droplet position, temperature may play an important role in detachment form filter which are not investigated in this study. It is important to note however that these results would need to be validated in real media.

Acknowledgements

The authors acknowledge the support of Australian Research Council under Linkage Grant (LP140100919) and Raschig GmbH, Germany. This work was also supported by the Pawsey Supercomputing Centre, Perth, WA with funding from the Australian Government and the Government of Western Australia.

References

[1] Mead-Hunter R, King AJC, Mullins BJ. Aerosol-mist coalescing filters – A review. Separation and Purification Technology 2014;133:484-506.

[2] Frising T, Thomas D, Bémer D, Contal P. Clogging of fibrous filters by liquid aerosol particles: Experimental and phenomenological modelling study. Chemical Engineering Science 2005;60:2751-62.

[3] Koponen A, Kandhai D, Hellén E, Alava M, Hoekstra A, Kataja M, et al. Permeability of Three-Dimensional Random Fiber Webs. Physical Review Letters 1998;80:716-9.

[4] Tafreshi HV, Rahman MA, Jaganathan S, Wang Q, Pourdeyhimi B. Analytical expressions for predicting permeability of bimodal fibrous porous media. Chemical Engineering Science 2009;64:1154-9.

[5] Fotovati S, Vahedi Tafreshi H, Pourdeyhimi B. Influence of fiber orientation distribution on performance of aerosol filtration media. Chemical Engineering Science 2010;65:5285-93.

[6] Spielman L, Goren SL. Model for predicting pressure drop and filtration efficiency in fibrous media. Environmental Science & Technology 1968;2:279-87.

[7] Mead-Hunter R, King AJC, Kasper G, Mullins BJ. Computational fluid dynamics (CFD) simulation of liquid aerosol coalescing filters. Journal of Aerosol Science 2013;61:36-49.

[8] Abishek S, King A, Narayanaswamy R. Dynamics of a Taylor bubble in steady and pulsatile co-current flow of Newtonian and shear-thinning liquids in a vertical tube. International Journal of Multiphase Flow 2015;74:148-64.

[9] Weller HG, Tabor G, Jasak H, Fureby C. A tensorial approach to computational continuum mechanics using object-oriented techniques. Computers in Physics 1998;12:620-31.

[10] Issa RI. Solution of the implicitly discretised fluid flow equations by operator-splitting. Journal of Computational Physics 1986;62:40-65.

[11] Pich J. Pressure characteristics of fibrous aerosol filters. Journal of Colloid and Interface Science 1971;37:912-7.

[12] Mullins B, Mead-Hunter R, King A. Simulating Plateau-Rayleigh instability and liquid reentrainment in a flow field using a VOF method. 2012.

[13] Darcy H. Les fontaines publiques de la ville de Dijon: exposition et application: Victor Dalmont; 1856.

[14] Andrade Jr J, Costa U, Almeida M, Makse H, Stanley H. Inertial effects on fluid flow through disordered porous media. Physical Review Letters 1999;82:5249.

[15] Scheidegger AE. The physics of flow through porous media. 1974.

[16] Noman R, Kalam MZ. Transition from laminar to non-darcy flow of gases in porous media. Advances in Core Evaluation: Accuracy and Precision in Reserves Estimation 1990:447-62.

[17] Hlushkou D, Tallarek U. Transition from creeping via viscous-inertial to turbulent flow in fixed beds. Journal of Chromatography A 2006;1126:70-85.

[18] Chapman RE. Geology and water: an introduction to fluid mechanics for geologists: Springer Science & Business Media; 2012.

[19] Mead-Hunter R, Mullins BJ, Becker T, Braddock RD. Evaluation of the force required to move a coalesced liquid droplet along a fiber. Langmuir : the ACS journal of surfaces and colloids 2011;27:227.